Riley, L. Schapiro, *Am. J. Hyg. Monogr. Ser.* **9** (1929).
18. A. C. Chandler, *Hookworm Disease* (Macmillan, New York, 1929), 429 pp.
19. T. A. Miller, *Adv. Parasitol.* **17**, 315 (1979).
20. ———, *J. Parasitol.* **52**, 512 (1962); *Immunology* **12**, 231 (1967); *Adv. Parasitol.* **9**, 153 (1971).
21. W. W. Cort and G. F. Otto, *Rev. Gastroenterol.* **7**, 2 (1940).
22. L. K. Martin, *Am. J. Trop. Med. Hyg.* **21**, 930 (1972).
23. J. G. Banwell and G. A. Schad, *Clin. Gastroenterol.* **7**, 129 (1978).
24. G. A. Schad and J. G. Banwell, in *Tropical and Geographic Medicine*, A. A. F. Mahmoud and K. S. Warren, Eds. (McGraw-Hill, New York, 1984), pp. 359–372.
25. H. H. Howard, *South. Med. J.* **18**, 668 (1925).
26. J. M. Andrews, *Am. J. Public Health* **32**, 282 (1942).
27. J. M. Andrews, *Ann. Intern. Med.* **17**, 891 (1942).
28. A. Bartlett and P. A. J. Ball, *Ann. Trop. Med. Parasitol.* **66**, 129 (1972); D. Wakelin, *Adv. Parasitol.* **16**, 219 (1978).
29. S. M. Lambert, *J. Trop. Med. Hyg.* **39**, 19 (1936).
30. K. S. Warren and A. A. F. Mahmoud, *Clin. Res.* **28**, 195 (1970).
31. K. S. Warren, *Annu. Rev. Public Health* **2**, 101 (1981).
32. R. M. Anderson and R. M. May, *Adv. Parasitol.*, in press.
33. Fieldwork in India was supported by foreign research agreement 01-027-01 and grant 5 RO 7 TW00141 from the U.S. Public Health Service. Data analysis was supported by a fellowship from the Welcome Trust. We thank G. Medley for assistance with data processing, C. Kirkpatrick for critical reading of the manuscript, and S. Shaw, S. Pharaoh and L. Hodges for assistance with the preparation of the manuscript.

25 June 1984; accepted 13 March 1985

Analysis of T-Cell Receptor Gene Rearrangement and Expression in Human Natural Killer Clones

Abstract. *A series of clones of human natural killer (NK) cells was characterized with respect to expression of the Ti α and Ti β genes of the T-cell receptor. $T11^+T3^+$ NK clones contained Ti α and Ti β RNA transcripts and expressed disulfide-linked heterodimers, demonstrating the presence of a functional T-cell receptor. In contrast, $T11^+T3^-$ NK clones expressed only 1.0-kilobase truncated Ti β transcripts, without a Ti α transcript and no detectable surface Ti protein. Since previous studies demonstrated that Ti β gene activation precedes Ti α gene activation in thymic ontogeny, the $T11^+T3^-$ NK cells appear to be derived from T-lineage precursors.*

Natural killer (NK) cells have been operationally defined as a population of cells capable of mediating direct cytotoxicity against various types of target cells without apparent prior immunization (*1*). Primarily because the cytotoxic specificity of NK cells is not restricted by or associated with expression of major histocompatibility complex (MHC) antigens on their target cells, NK cells have been thought to be functionally distinct from cytotoxic T lymphocytes. In peripheral blood, NK cells appear to be a morphologically homogeneous population of large granular lymphocytes (LGL) that can be distinguished and separated from conventional T cells by their differing physical characteristics (*2*). Nevertheless, the lineage of NK cells has not been established since they express both T lymphocyte– and myeloid-associated cell surface antigens. Moreover, the structural basis by which these cells exert their cytotoxic function has not been defined for most of the NK active cells.

In order to analyze NK cell function and heterogeneity, we and others have developed and characterized monoclonal NK cell lines from normal peripheral blood (*3*). This is possible because NK cells proliferate in response to nonspecific stimulation, and this proliferation can be maintained by interleukin-2. Using these techniques, we were able to select a series of NK clones solely on the basis of their ability to mediate cytotoxicity against various types of target cells without prior sensitization. Previous characterization of these NK clones has shown that they can maintain a stable phenotype and cytotoxic function after prolonged periods of culture in vitro. Moreover, these NK clones appear to reflect accurately the phenotypic and functional diversity of NK cells in unstimulated peripheral blood. In the present experiments, we used DNA probes for the Ti α (*4*) and Ti β (*5*) genes of the T-cell receptor to analyze various NK clones for the presence of specific T-cell lineage rearrangements as well as expression of T-cell receptor gene products. These studies were undertaken to further characterize the derivation of NK cells and to analyze the structural basis for the cytotoxic function of these cells.

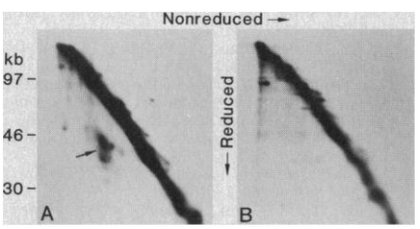

Fig. 1. Two-dimensional SDS-PAGE of NK clones labeled at surface membranes with ^{125}I. (A) JT9 cells. (B) JT3 cells. Lymphoid cells were externally labeled with ^{125}I-labeled lactoperoxidase, and total cell lysates from 5×10^6 to 10×10^6 cells were analyzed by modification of the procedure described by Goding and Harris (*10, 11*). Lysates were first resolved under nonreducing conditions in a 10 percent acrylamide Laemmli tube gel. When the bromophenol blue marker reached the bottom of the tube, the gel was removed and equilibrated for 1 hour at 25°C in sample buffer containing 10 percent 2-mercaptoethanol and 100 m*M* dithiothreitol. Samples were then subjected to electrophoresis in the second dimension under reducing conditions in a 10 percent acrylamide Laemmli slab gel. Gels were fixed and autoradiographed with intensifying screens and Kodak X-R5 film at −70°C for 48 hours. The arrow in (A) indicates the position of the disulfide-linked heterodimer. A similar spot is not detectable in (B).

The phenotype of the NK clones used in our studies is summarized in Table 1. Clones JT3 and JT_B18 represent the phenotype of most of the NK cells in peripheral blood (*6*). These cells express T11/E rosette antigen and NKH1, a pan-NK cell antigen, but do not express T3, T4, or T8 antigens. Although these two clones have a similar phenotype, they were derived from different individuals, and only JT3 cells express NKH2 antigen—another marker associated with LGL in peripheral blood (*6*). Clones JT3, JT9, and JT10 were derived at separate times from the same individual, but JT9 and JT10, in contrast to JT3, have a mature T-cell phenotype ($T3^+$, $T8^+$, $T11^+$). Unlike most T lymphocytes, however, these cells express NKH1 antigen and kill a wide variety of target cells including K562. Cytotoxicity of JT9 and JT10 cells is not MHC-restricted and cannot be blocked by monoclonal antibodies specific for T8 structures or for histocompatibility antigen class I or class II products (*7*). Clones JT9 and JT10 demonstrate an identical target specificity to each other, and both express a 90-kilodalton (kD) clonotypic disulfide-linked heterodimeric receptor (NKTa) that is linked to surface T3 antigen and appears to be the product of functional T-cell receptor genes (*8*). Cytotoxicity of JT9 and JT10 cells can be blocked at the effector cell level by monoclonal antibodies specific for NKTa or T3 antigens and at the target cell level by monoclonal antibodies specific to TNK_{TAR}, a 140-kD glycoprotein that is widely expressed on normal lymphoid and hematopoietic cells after cell activation (*9*). Clone CNK3 was derived from a different individual and also has a mature T-cell phenotype ($T3^+$,$T8^+$, and $T11^+$). Furthermore, its cytotoxicity is also blocked by antibody to T3. Unlike JT9 and JT10, these cells express NKH2 antigen and do not express NKTa.

The possibility that NK clones lacking T3 express a disulfide-linked heterodi-

meric T-cell receptor–like structure, was examined by use of two-dimensional sodium dodecyl sulfate–polyacrylamide gel electrophoresis (SDS-PAGE) to analyze total lysates from cells surface-labeled with ^{125}I. Surface-labeled cell lysates were separated in one dimension under nonreducing conditions and then resolved in a second dimension under reducing conditions, as described by Goding and Harris (*10*) and Acuto *et al.* (*11*). Under these conditions, T-cell receptor–like structures that are disulfide-linked heterodimers can be separated from the vast majority of membrane proteins, which migrate identically in both reducing and nonreducing conditions. JT9 cells that were earlier shown to express a 90-kD disulfide-linked heterodimer have a set of off-diagonal spots at approximately 49- and 43-kD sizes consistent with known Ti α and Ti β proteins, respectively. (Fig. 1A). In contrast, JT3 cells that are representative of $T3^-$ NK clones do not express such a structure in this molecular weight range, although at least a single off-diagonal spot is evident elsewhere (for example, at approximately 38 kD). These data indicate that at least some $T11^+T3^-$ NK clones must use a structure distinct from that of T3-Ti in the recognition process.

To further characterize $T3^+$ and $T3^-$ NK populations, we used complementary DNA (cDNA) probes specific for the Ti β and Ti α subunits of the human T-cell receptor (*12, 13*). Individual cytoplasmic RNA's were extracted from each clonal population, separated according to size with agarose gel electrophoresis, and subsequently analyzed by the Northern blot technique. As shown in Fig. 2 for the mature T-cell tumor REX (lane E), two different species of Ti β RNA can be identified—the prevalent species of approximately 1.3 kilobases (kb) and the much less abundant species at 1.0 kb. Whereas the 1.3-kb form of the message represents the complete transcript resulting from joining of dispersed germline V and D segments to J-C segments (variable and diversity regions to joining and constant regions), the 1.0-kb message is a truncated D-J-C transcript (*14*). As shown in lane H of Fig. 2, the $T3^+$ NK clone JT9 expresses both 1.3- and 1.0-kb Ti β transcripts. In contrast, the $T3^-$ NK clones JT_B18 and JT3 (lanes F and G) express the 1.0-kb form of Ti β transcripts in the absence of the 1.3-kb form. Analysis of Ti α RNA in these cells shows that REX (lane A) and JT9 (lane D) both express 1.6- and 1.3-kb transcripts whereas, in contrast, the $T3^-$ clones JT_B18 and JT3 (lanes B and C) lack both message sizes.

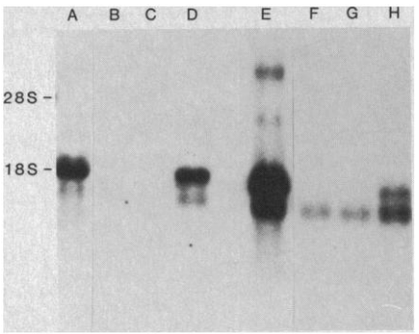

Fig. 2. Northern analysis of RNA from NK clones with Ti Cα and Ti Cβ probes. RNA was prepared from cell pellets by lysis with NP-40 in the presence of 10 m*M* vanadyl ribonucleoside (BRL), removal of nuclei by centrifugation, proteinase K digestion, phenol extraction, and ethanol precipitation (the last two procedures being repeated twice). The material was treated with formaldehyde and run on agarose gels containing formaldehyde. Before transfer to GeneScreen Plus, gels were soaked in 20× standard sodium citrate (SSC) for 30 minutes. After transfer, membranes were baked at 80°C for 2 hours to inactivate formaldehyde, hybridized first in plaque screen buffer (PSB), and then hybridized overnight at 65°C in PSB containing Ti Cα (lanes A to D) or Ti Cβ (lanes E to H) probes at 3×10^6 to 5×10^6 cpm/ml. Membranes were then washed in PSB at 65°C for 45 minutes and in plaque screen salt for 45 minutes at 65°C and exposed to Kodak XR x-ray film for 24 to 72 hours. The cloning of DNA segments used for generating these probes is described elsewhere (*12, 13*). The Ti Cβ probe was derived by digesting plasmid pCβ REX with Eco RI and Bgl II to yield a fragment of about 800 bases long containing the constant region of Ti β. Lambda α REX, a λ gt10 clone containing partial Ti α cDNA segments, was digested with Eco RI and MnlI λ to yield a fragment approximately 400 bases long and containing about 100 bases of the Ti α V region and an additional 300 bases of Ti α J and C regions. The appropriate inserts were run on low-melting-point agarose gels (BRL). The bands were removed, diluted with tris-EDTA buffer, and labeled directly to high specific activity with the use of DNA polymerase I large-fragment (New England Biolabs) and random primers (P-L) following a protocol by Feinberg and Vogelstein (*20*). Lanes contained approximately 8 μg each of RNA from different cells as follows: (lanes A and E) REX; (lanes B and F) JT_B18; (lanes C and G) JT3; and (lanes D and H) JT9.

Since active T-cell receptor genes result from joining DNA fragments that are discontiguous in the germline, we examined individual NK clones with regard to their Ti β gene rearrangement. For this purpose, we made use of the Ti β probe, which hybridizes equally well to the germline Cβ1 and Cβ2 segments, respectively (*12*). Genomic DNA was digested with one or another restriction endonuclease, size-fractionated by agarose gel electrophoresis, and hybridized with ^{32}P-labeled Ti Cβ REX probe. Figure 3 shows the germline pattern of the B lymphoblastoid line Laz 461 (lane A)

Table 1. Characteristics of natural killer clones. Expression of each antigen was determined for each clone by indirect immunofluorescence assay using specific monoclonal antibodies and fluorescein-conjugated goat antibody to murine immunoglobulin (GM-FITC) (Tago, Burlingame, California). After removal of excess of GM-FITC, cells were fixed with 1 percent formaldehyde in PBS, and 10,000 cells were analyzed on a flow cytometer (Epics V or Epics C, Coulter Electronics). In each instance, reactivity with a specific monoclonal antibody was compared to reactivity with a nonspecific murine antibody and GM-FITC. Cells were considered to be negative if fewer than 10 percent of the cells were reactive with monoclonal antibody. In all cases of positive reactivity, more than 80 percent of cells were reactive with monoclonal antibody. Each NK clone was derived from normal peripheral blood by limiting dilution and was selected primarily for its ability to kill K562 target cells without prior immunization (*3*). Each clone was subsequently shown to kill a wide variety of unrelated target cells, some of which do not express either class I or class II major histocompatibility molecules. In addition, cytotoxicity of these clones cannot be blocked by monoclonal antibodies specific for class I or class II MHC products (*8*). Clones JT9 and JT10 have been determined to be specific for a cell surface glycoprotein of 140 kD expressed following cell activation termed TNK_{TAR} (*9*).

NK clone	Antigen expression							Cytotoxic specificity	Reference
	T3	T4	T8	T11	NKH1	NKH2	NKTa		
JT3	−	−	−	+	+	+	−	Non-MHC	(*3*)
JT_B18	−	−	−	+	+	−	−	Non-MHC	(*3*)
JT9	+*	−	+	+	+	−	+	140-kD TNK_{TAR}	(*9*)
JT10	+	−	+	+	+	−	+	140-kD TNK_{TAR}	(*9*)
CNK3	+	−	+	+	+	+	−	Non-MHC	

*Cytotoxicity of $T3^+$ clones JT9, JT10, and CNK3 can be blocked by incubation with monoclonal antibody to T3 (*8, 9*). Cytotoxicity of $T3^-$ clones is not inhibited by anti-T3.

and, for comparison, a rearranged Cβ1 locus pattern of the T4$^+$ T-cell clone AC3 (lane B). Since not all restriction enzymes will provide detectable rearrangements, both Eco RI digestion (which detects Cβ1 rearrangement) and Bam HI digestion (which detects Cβ1 and Cβ2 rearrangements) were performed for each cellular DNA preparation. Lane A shows the germline 10.2-kb Cβ1 and 4.0-kb Cβ2 bands in the Eco RI digest and a single 24-kb fragment containing both Cβ1 and Cβ2 loci in the Bam HI digest of Laz 461. In contrast, a rearranged Cβ1 allele is detected in the Eco RI digest of AC3 (lane B) and further confirmed in the Bam HI digest as well. In the case of T3$^+$ NK clones, DNA from CNK3 (lane C) shows a rearranged Cβ fragment in the Eco RI digest, whereas JT10 (lane E) and JT9 (lane G) show a rearrangement in the Bam HI digest. Since an Eco RI restriction site exists between the J and C region of the Cβ2 locus, this finding would suggest that both JT9 and JT10 use Cβ2 and CNK3 uses Cβ1.

Rearrangements, as evidenced by changes in sizes of hybridizing restriction fragments, were less evident in either Cβ locus of the T3$^-$ clones JT3 (lane F) and JT$_B$18 (lane D). However, a slight difference in mobility of the Cβ1 band in the Eco RI digest of JT3 and an additional band in the Bam HI digest of JT$_B$18 suggests that some rearrangement may be occurring. Since transcription of the 1.0-kb Ti β message is detected in these cells in Northern analysis, the most likely explanation for these alterations from the germline pattern in JT3 and JT$_B$18 may relate to joining of D and J segments that are separated by approximately 500 nucleotides in the germline array before rearrangement. For further clarification of this type of rearrangement, studies with probes specific for the J locus and other restriction endonucleases are needed. In any event, our results indicate that T3$^+$ NK cells have a clearly detectable Ti Cβ rearrangement, further supporting the view that these cells use the same genetic mechanisms as other T cells to generate an active T-cell receptor structure. Although it would be of interest to examine these same cells for Ti α gene rearrangements, the large distance (in excess of 10 kb) between the J and C regions makes it difficult to detect similar rearrangements with a Ti α C-region probe.

Taken together, our data on the rearrangement and expression of T-cell receptor genes in NK clones appear to reflect the heterogeneity of cells capable of mediating this unusual cytolytic capacity. Previous characterization of NK

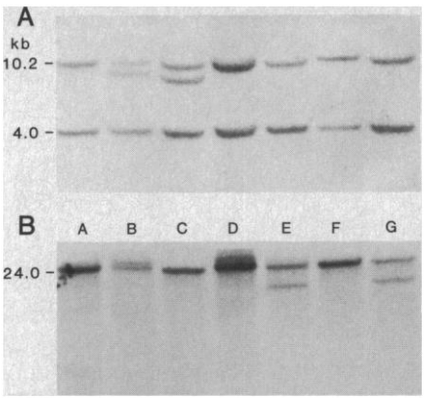

Fig. 3. Southern blot analysis of NK clones with the TiC β probe. DNA from seven cell lines was digested with either (A) Eco RI or (B) Bam HI, fractionated on 0.8 percent agarose gels, transferred to nitrocellulose membranes, and hybridized with ^{32}P-labeled TiC β probe (*12*). The filters were hybridized in 6× standard saline phosphate EDTA (SSPE) at 68°C overnight, washed in 1× SSPE plus 0.1 percent SDS at room temperature for 30 minutes, 0.5× SSPE plus 0.1 percent SDS at 68°C for 30 minutes, and then twice in 0.2× SSPE plus 0.1 percent SDS at 68°C for 60 minutes; and membranes were exposed to Kodak XR film overnight. Lanes contained approximately 10 μg of DNA from different cells as follows: (lane A) Laz 461; (lane B) T cell clone AC3; (lane C) CNK3; (lane D) JT$_B$18; (lane E) JT10; (lane F) JT3; and (lane G) JT9.

clones with a mature T3$^+$ T-cell phenotype, such as clones JT9 and CNK3, has indicated that cells of this type express a T-cell receptor–like molecule and that, although their cytotoxic specificity is not MHC restricted, it is mediated through a specific receptor-antigen interaction (*8*). This hypothesis is supported by our finding in these cells: (i) clonal Ti β gene rearrangements, (ii) expression of both 1.6-kb Ti α and 1.3-kb Ti β messenger RNA (mRNA) in the cytoplasm, and (iii) the surface expression of Ti-like heterodimers as detected by two-dimensional SDS-PAGE of ^{125}I-labeled proteins. Although both JT9 and CNK3 cells have NK-like activity, only JT9 cells are reactive with antibody to NKTa, and these clones have distinct patterns of cytotoxicity when tested against a large panel of different target cells. This suggests that T3$^+$ NK clones can have distinct receptor-mediated specificities, and this is further supported by the finding that these two clones have different Ti β gene rearrangements. Earlier studies have shown that clones JT9 and JT10, which were derived independently from the same individual, express the same T3-associated 90-kd disulfide-linked heterodimer NKTa antigen, have an identical pattern of cytotoxic activity, and can be blocked by monoclonal antibody to TNK$_{TAR}$ at the target level (*9*). In the present studies, indistinguishable patterns of Ti β gene rearrangements observed with these clones further indicate that they express the same T-cell receptor structure.

Although NK clones such as JT9, JT10, and CNK3 are phenotypically and functionally related to mature T cells, they cannot be considered representative of most NK cells since, in unstimulated peripheral blood, more than 80 percent of NK cells express T11/E rosette antigen but fewer than 5 percent express T3, and monoclonal antibodies to T3 do not inhibit the NK activity of these cells. In contrast, clones JT3 and JT$_B$18, which express T11 but not T3, appear to be representative of most NK cells. The recognition structure (or structures) imparting specificity to their cytotoxic function has not been determined. The results of two-dimensional SDS-PAGE of surface-labeled proteins indicate that it is not a Ti-like receptor structure. This notion is also supported by the lack of detectable Ti α gene mRNA expression.

Nevertheless, it is particularly interesting that these T3$^-$ NK cells express the 1.0-kb form of the Ti β message in the absence of the 1.3-kb Ti β message or any form of Ti α. Such T11$^+$T3$^-$ NK clones appear to be analogous to early thymocytes (stages I and II), which also express T11 on their surface but lack other T-lineage structures including T3$^-$ Ti. Similarly, early thymocytes express no Ti α mRNA, yet express 1.0-kb Ti β transcripts with little or no 1.3-kb Ti β transcripts (*13*). Since D and J segments are apparently joined in T-cell loci and in B-cell immunoglobulin H loci before the joining of V to D, this transcript size also implies an early state of differentiation (*15*). Furthermore, transcriptional analysis of normal thymocytes and thymic tumors supports the view that Ti β gene activation occurs before Ti α gene activation (*13*). Our present findings indicate that T11$^+$ T3$^-$ NK clones such as JT3 and JT$_B$18 may be representative of early thymic lineage cells, having undergone Ti β D-J joining events only. Of course, we cannot exclude the possibility that D-J joining events within the Ti β gene locus are not restricted to the T lineage.

If the Ti α-β heterodimer is not expressed on T3$^-$ NK cells, then what structure serves as their recognition site? Because of the importance of the T11 structure in triggering early T3$^-$ stage I and stage II thymocytes (*16*) and T11$^+$T3$^-$ NK clones (*17*) as well as mature T lymphocytes (*18*), the present results suggest that the T11 molecule may be important in the activation of NK cells in general and may serve as the receptor for a putative NK target antigen

on NK-susceptible populations. In this respect, it is important to determine whether peptide variability exists within the T11 molecule.

Although the recent finding of a third T-cell–specific cDNA clone encoding a putative nonglycosylated T-cell receptor–like molecule, termed γ, suggested that the γ gene and its product may be operational in $T3^-T11^+$ NK populations as a receptor (*19*), this possibility has been excluded by transcriptional analysis. No γ mRNA sequences were detected in two $T3^-T11^+$ clones examined.

JEROME RITZ
THOMAS J. CAMPEN
REINHOLD E. SCHMIDT
HANS DIETER ROYER
THIERRY HERCEND*
REBECCA E. HUSSEY
ELLIS L. REINHERZ

Division of Tumor Immunology, Dana-Farber Cancer Institute, and *Departments of Medicine and Pathology, Harvard Medical School, Boston, Massachusetts 02115*

References and Notes

1. R. B. Herberman and J. R. Ortaldo, *Science* **214**, 24 (1981); G. Trinchieri and B. Perussia, *Lab. Invest.* **50**, 489 (1984).
2. T. Timonen, J. R. Ortaldo, R. B. Herberman, *J. Exp. Med.* **153**, 569 (1981).
3. T. Hercend *et al.*, *J. Immunol.* **129**, 1299 (1982); T. Hercend *et al.*, *Nature (London)* **301**, 158 (1983); R. E. Schmidt *et al.*, *J. Immunol.*, in press; G. Dennert, G. Yogeeswaran, S. Yamagata, *J. Exp. Med.* **153**, 545 (1981); J. F. Warner and G. Dennert, *Nature (London)* **300**, 31 (1982); P. Allavena and J. R. Ortaldo, *J. Immunol.* **132**, 2363 (1984).
4. Y. Chien *et al.*, *Nature (London)* **312**, 31 (1984); M. Fabbi *et al.*, *ibid.*, p. 269; C. H. Hannum *et al.*, *ibid.*, p. 65; H. Saito *et al.*, *ibid.*, p. 36; G. Siu *et al.*, *ibid.* **311**, 344 (1984).
5. O. Acuto *et al.*, *Proc. Natl. Acad. Sci. U.S.A.* **81**, 3851 (1984); N. Gascoigne *et al.*, *Nature (London)* **310**, 387 (1984); S. M. Hedrick *et al.*, *ibid.* **308**, 149 (1984); G. Siu *et al.*, *Cell* **37**, 393 (1984); Y. Yanagi *et al.*, *Nature (London)* **308**, 145 (1984); Y. Yoshikai *et al.*, *ibid.* **312**, 521 (1984); P. E. Barker *et al.*, *Science* **226**, 348 (1984).
6. J. R. Ortaldo *et al.*, *J. Immunol.* **127**, 2401 (1981); B. Perussia *et al.*, *ibid.* **130**, 2133 (1983); L. L. Lanier *et al.*, *ibid.* **131**, 1789 (1981); T. Hercend *et al.*, *J. Clin. Invest.*, in press.
7. S. C. Meuer *et al.*, *Science* **218**, 471 (1982).
8. T. Hercend *et al.*, *J. Exp. Med.* **158**, 1547 (1983); S. C. Meuer *et al.*, *Science* **222**, 1239 (1983).
9. T. Hercend *et al.*, *Eur. J. Immunol.* **14**, 844 (1984).
10. J. W. Goding and A. W. Harris, *Proc. Natl. Acad. Sci. U.S.A.* **78**, 4530 (1981).
11. O. Acuto *et al.*, *Cell* **34**, 717 (1983).
12. H. D. Royer *et al.*, *ibid.* **39**, 261 (1984).
13. H. D. Royer *et al.*, *Proc. Natl. Acad. Sci. U.S.A.*, in press.
14. O. Acuto *et al.*, *J. Exp. Med.*, in press.
15. F. Alt *et al.*, *EMBO J.* **3**, 1209 (1984).
16. D. A. Fox *et al.*, *J. Immunol.* **134**, 330 (1985).
17. R. E. Schmidt *et al.*, *ibid.*, in press.
18. S. C. Meuer *et al.*, *Cell* **36**, 897 (1984).
19. H. Saito *et al.*, *Nature (London)* **309**, 757 (1984); D. M. Krantz *et al.*, *ibid.* **313**, 752 (1985); D. Raulet *et al.*, *ibid.* **314**, 103 (1985).
20. A. P. Feinberg and B. Vogelstein, *Anal. Biochem.* **132**, 6 (1983).
21. Supported in part by NIH grants CA 34183, AI 19807, and AI 21226. J.R. is a scholar of the Leukemia Society of America; T.C. is a fellow of the Leukemia Society of America; R.S. is a recipient of a fellowship (Schm 596/1-1) from the Deutsche Forschungsgemeinschaft; T.H. is a special fellow of the Leukemia Society of America.
* Present address: Cellular Biology Unit, Institut Gustave-Roussy, Villejuif, France.

18 March 1985; accepted 20 May 1985

Imaging Elemental Distribution and Ion Transport in Cultured Cells with Ion Microscopy

Abstract. *Both elemental distribution and ion transport in cultured cells have been imaged by ion microscopy. Morphological and chemical information was obtained with a spatial resolution of approximately 0.5 μm for sodium, potassium, calcium, and magnesium in freeze-fixed, cryofractured, and freeze-dried normal rat kidney cells and Chinese hamster ovary cells. Ion transport was successfully demonstrated by imaging Na^+-K^+ fluxes after the inhibition of Na^+- and K^+-dependent adenosine triphosphatase with ouabain. This method allows measurements of elemental (isotopic) distribution to be related to cell morphology, thereby providing the means for studying ion distribution and ion transport under different physiological, pathological, and toxicological conditions in cell culture systems.*

Most cells expend much of their energy in maintaining ionic balance, and ions play an important role in intracellular regulatory events. Cells grown in cultures provide an excellent model for studying the distribution and transport of ions under normal and pathological conditions. Ion microscopy, a technique that provides visual ion images with cell morphology, is ideally suited for such studies.

Ion microscopy is based on secondary ion mass spectrometry (SIMS), and the details of the technique have been reported (*1*, *2*). In brief, the sample to be analyzed is mounted on a conducting substrate (silicon wafers or tantalum disks, for example) and placed in the high-vacuum (10^{-7} to 10^{-8} torr) sample chamber of the ion microscope. The sample is then bombarded with a primary ion beam (O_2^+, Ar^+, and so forth), which removes the top two or three atomic layers of the sample surface by sputtering. A fraction of these atoms leave the surface as ions. These sputtered secondary ions are then accelerated into a double-focusing mass spectrometer that separates them according to their mass-to-charge ratio. The ion optics of the instrument preserves the spatial distribution of the emitted secondary ions through the mass spectrometer so that a one-to-one correspondence is maintained between the position of a sputtered ion leaving the sample surface and its position in the final mass-resolved ion image. This final magnified ion image reveals the spatial distribution of any selected element (in both free and bonded states) within an area up to 400 μm in diameter with a spatial resolution of ~0.5 μm. A micro-channelplate detector, coupled with a fluorescent screen, converts the ion image into a visible image. The visible ion images produced in this fashion can be recorded directly from the fluorescent screen of the ion microscope with a 35-mm camera. Because multielement distributions can be evaluated from the same cells in this way, we have been able to image the

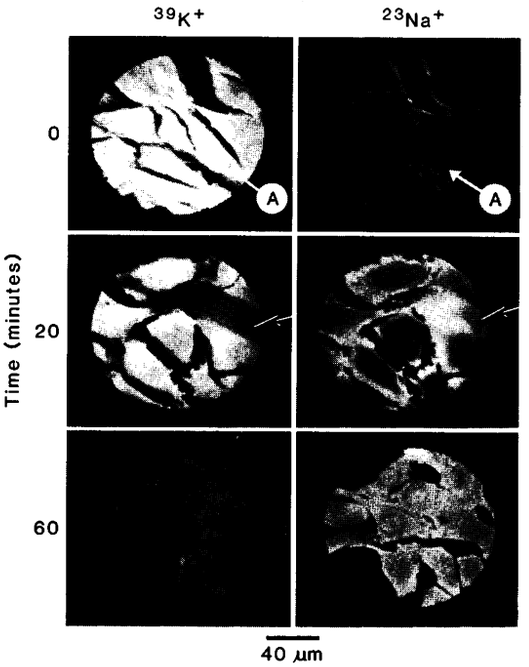

Fig. 1. Imaging Na^+-K^+ ion transport in NRK cells after inhibition of the Na^+- and K^+-dependent adenosine triphosphatase of the plasma membrane with a specific inhibitor, ouabain. Time (in minutes) indicates the exposure of cells to ouabain. The ion images of potassium ($^{39}K^+$) are in the left column and the corresponding sodium ($^{23}Na^+$) images are on the right for each treatment. At 0 minutes, the arrow marked A indicates the same cell. Brightness indicates relative ion intensities. A dead cell with high sodium and very low potassium is indicated by the arrow in the images made after 20 minutes of treatment with ouabain.